

# Effect of Fe composition on the superconducting properties ( $T_c$ , $H_{c2}$ and $H_{irr}$ ) of $Fe_xSe_{1/2}Te_{1/2}$ ( $x = 0.95, 1.00, 1.05$ and $1.10$ )

Sudesh,<sup>1</sup> S. Rani,<sup>1</sup> S. Das,<sup>3</sup> R. Rawat,<sup>2</sup> C. Bernhard,<sup>3</sup> and G. D. Varma<sup>1,a)</sup>

<sup>1</sup>Department of Physics, Indian Institute of Technology Roorkee, Roorkee-247667, India

<sup>2</sup>UGC-DAE C.S.R., University Campus, Khandwa Road, Indore-452001, India

<sup>3</sup>Department of Physics and Fribourg Centre for Nanomaterials-FriMat, University of Fribourg, Fribourg, Switzerland

In the present work, we have studied the effect of Fe composition on the superconducting properties, such as transition temperature ( $T_c$ ), upper critical field ( $H_{c2}$ ), and irreversibility field ( $H_{irr}$ ) of  $FeSe_{1/2}Te_{1/2}$ . The polycrystalline samples have been prepared via solid state reaction route with nominal compositions  $Fe_xSe_{1/2}Te_{1/2}$  ( $x = 0.95, 1.00, 1.05$  and  $1.10$ ). The x-ray diffraction results show the presence of tetragonal  $\alpha$ -FeSe phase with the  $p4/nmm$  space group symmetry in all the samples. The zero resistance temperatures,  $T_c^{zero}$ , measured in zero magnetic field, have been found to be 10.0, 12.4, 12.3, and 11.7 K for  $x = 0.95, 1.00, 1.05$ , and  $1.10$ , respectively. The temperature dependence of  $H_{c2}(T)$  and  $H_{irr}(T)$  have been calculated from the magnetoresistance data using the criteria of 90% and 10% of normal state resistivity ( $\rho_n$ ) values, respectively. The values of  $H_{c2}(0)$  are 121.3 T, 142.8 T, 82.7 T, and 79.3 T for  $x = 0.95, 1.00, 1.05$ , and  $1.10$ , respectively. The possible reasons for the variation of superconducting properties with Fe composition ( $x$ ) have been described and discussed in this paper.

## I. INTRODUCTION

The discovery of superconductivity in Fe-based doped LaFeAsO (Ref. 1) with  $T_c = 26$  K has stimulated further research into this area. To date the superconducting critical temperature,  $T_c$  has been raised to 56 K by replacing La with other rare earth elements such as Ce, Pr, Nd, Sm or Gd. The FeAs-based family has further been expanded to include  $AE_{1-x}A_xFe_2As_2$ ,<sup>2,3</sup>  $AFeAs$ ,<sup>3,4</sup>  $FeSe$ ,<sup>5</sup> and  $AFe_2Se_2$ <sup>6</sup> ( $A$ =Alkali metal and  $AE$ =Alkaline Earth metal). It has been shown<sup>7</sup> that structural, electronic, and magnetic properties present in pnictides are also present in FeSe except that it has a lower critical temperature,  $T_c \sim 8$  K. The absence of poisonous As atom and simplified structure of FeSe compound gives an opportunity to carry out the study on this system to understand the underlying phenomenon which leads to superconductivity in these layered compounds. Among various substitutions,<sup>8</sup> 50% substitution of Te at the Se site has shown a maximum  $T_c$  of around 15K. Despite having crystal structure similar to pnictides, the interstitial sites of the (Te, Se) layers in the FeSe compounds allow partial occupation of iron, resulting into non-stoichiometric composition  $Fe_{1+y}(Te, Se)$ ,<sup>9</sup> which shows a significant effect on the superconducting properties of this compound. Recently, it has been reported that the superconducting and magnetic properties of  $Fe_ySe_xTe_{1-x}$  not only depend on the Se-Te ratio but also strongly on the Fe content.<sup>10</sup> In the present work, we have investigated the effect of variation of Fe-content on the superconducting transition temperature ( $T_c$ ), upper critical

field ( $H_{c2}(0)$ ) and irreversibility field ( $H_{irr}$ ) of polycrystalline  $Fe_xSe_{1/2}Te_{1/2}$  ( $x = 0.95, 1.00, 1.05$  and  $1.10$ ) samples.

## II. EXPERIMENT

Polycrystalline samples with nominal compositions  $Fe_xSe_{1/2}Te_{1/2}$  ( $x = 0.95, 1.00, 1.05, 1.10$ ) were synthesized using a two-step solid state reaction method. The appropriate amount of Fe (Alfa Aesar 99.99%), Se (Alfa Aesar 99.9%), and Te (Alfa Aesar 99.99%) were weighed and ground in a glovebox having Ar atmosphere. The resulting powder was pressed into rectangular pellets. The pellets were sealed in an evacuated ( $10^{-5}$  Torr) quartz tube and kept in the furnace for 20 h at 650 °C. The samples obtained were reground and again pressed into pellets. After sealing them again in evacuated quartz tube, the samples were sintered at 700 °C for 30 h followed by annealing at 400 °C for 30 h to stabilize the tetragonal PbO structure. Samples thus obtained were characterized for phase and structure by means of X-ray diffraction (XRD). Resistivity measurements were carried out using the four probe technique in the temperature range 3–300 K in applied magnetic fields (0–8 T) using the physical property measuring system (PPMS). The DC magnetic measurements were carried out by a vibrating sample magnetometer in a PPMS (Quantum Design). The elemental analysis of the samples was carried out using energy-dispersive X-ray analyzer (EDAX' TSL, AMETEK) coupled with the FE-SEM. EDAX data indicate that all samples are in proper composition within the experimental error (see Table I).

## III. RESULTS AND DISCUSSION

Figure 1 shows the X-ray diffraction patterns of the samples  $Fe_xSe_{1/2}Te_{1/2}$ ,  $x = 0.95, 1.00, 1.05$ , and  $1.10$  recorded at

<sup>a)</sup>Author to whom correspondence should be addressed. Electronic mail: gvarfph@iitr.ernet.in.

TABLE I. Compositional analysis using EDAX.

Nominal	EDAX
$\text{Fe}_{0.95}\text{Se}_{0.50}\text{Te}_{0.50}$	$\text{Fe}_{0.94}\text{Se}_{0.59}\text{Te}_{0.47}$
$\text{Fe}_{1.00}\text{Se}_{0.50}\text{Te}_{0.50}$	$\text{Fe}_{0.98}\text{Se}_{0.56}\text{Te}_{0.46}$
$\text{Fe}_{1.05}\text{Se}_{0.50}\text{Te}_{0.50}$	$\text{Fe}_{1.03}\text{Se}_{0.55}\text{Te}_{0.42}$
$\text{Fe}_{1.10}\text{Se}_{0.50}\text{Te}_{0.50}$	$\text{Fe}_{1.07}\text{Se}_{0.49}\text{Te}_{0.44}$

room temperature. The majority of the diffraction peaks have been indexed with the tetragonal structure having space group  $P4/nmm$ . In the XRD pattern of the Fe deficient  $\text{Fe}_{0.95}\text{Se}_{1/2}\text{Te}_{1/2}$  sample few XRD peaks correspond to impurity phases  $\text{Fe}_7\text{Se}_8$ . The peaks corresponding to  $\text{Fe}_7\text{Se}_8$  phase disappear with increasing Fe content in the sample. The variations of lattice constants  $a$  and  $c$  with Fe content in the samples are shown in the inset of Fig. 1. The temperature dependence of resistivity ( $\rho$ ) of  $\text{Fe}_x\text{Se}_{1/2}\text{Te}_{1/2}$  ( $x = 0.95, 1.00, 1.05,$  and  $1.10$ ) samples is shown in Fig. 2. The  $\rho$ - $T$  plots of samples  $x = 0.95, 1.00,$  and  $1.05$  show curved temperature dependence in the normal state above the superconducting transition temperature. This kind of behavior in temperature dependence of resistivity has also been seen in the other Te doped FeSe compounds.<sup>11</sup> The sample  $\text{Fe}_{1.10}\text{Se}_{1/2}\text{Te}_{1/2}$ , however, shows semiconducting behavior in the whole temperature region above  $T_c^{\text{onset}}$ . A logarithmic behavior is seen in  $\text{Fe}_{1.10}\text{Se}_{1/2}\text{Te}_{1/2}$  below 100 K in the semiconducting region before the onset of superconductivity which indicate the presence of weakly localized electronic states.<sup>12</sup> This shows that the increased Fe content gives rise to weakly localized electronic states in the system. From the zero field  $\rho$ - $T$  plots, the zero resistance temperatures,  $T_c^{\text{zero}}$ , are  $\sim 10.0, 12.4, 12.3,$  and  $11.7$  K and the superconducting onset temperature,  $T_c^{\text{onset}}$

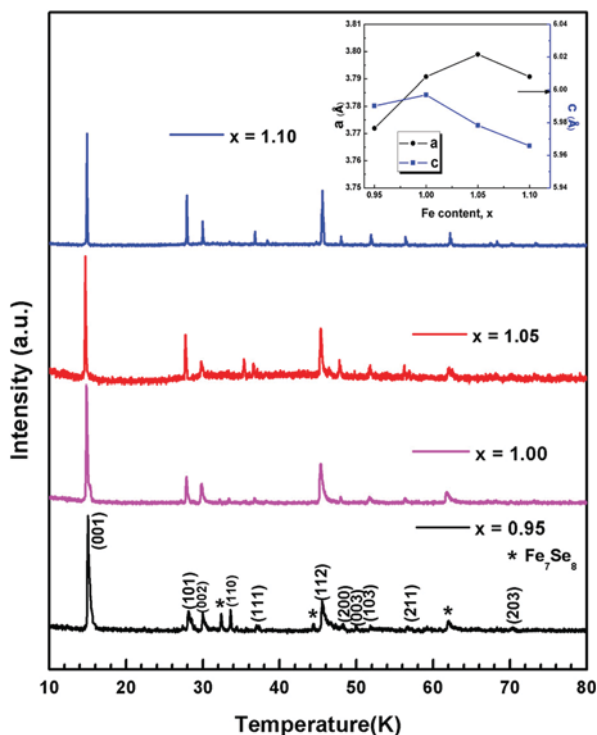


FIG. 1. (Color online) X-ray diffraction patterns of  $\text{Fe}_x\text{Se}_{1/2}\text{Te}_{1/2}$  ( $x = 0.95, 1.00, 1.05,$  and  $1.10$ ), \* represents the impurity peaks of  $\text{Fe}_7\text{Se}_8$ . Inset shows the variation of lattice parameters  $a$  and  $c$  with Fe content.

are  $\sim 14.2, 14.4, 14.3,$  and  $14.1$  K for  $x = 0.95, 1.00, 1.05,$  and  $1.10$ , respectively. We see that both the  $T_c^{\text{onset}}$  and  $T_c^{\text{zero}}$  are maximum for the composition  $x = 1.00$  and decrease for the samples with higher Fe content. Almost the same values of  $T_c^{\text{onset}}$  have been found from the onset of diamagnetic signals in the temperature dependent magnetization (field cooled (FC)) measured in an applied magnetic field of 30 Oe. However, the samples with  $x > 1.00$  show very weak diamagnetic signals as shown in the inset (b) of Fig. 2. Thus, the magnetic measurement shows that the samples with  $x > 1.00$  have small superconducting volume as compared to the samples with  $x \leq 1.00$ . Similar results have been reported by other groups.<sup>12,13</sup> This shows that the superconductivity in the  $\text{Fe}_x(\text{Se},\text{Te})$  compound depends strongly on the Fe content. From Fig. 2 it is also seen that the normal state resistivity continuously decreases with increasing the Fe content. This is possibly due to the excess Fe present at the octahedral sites which acts as electron donor and thus increasing the charge carrier density and hence decreasing the resistivity.<sup>14</sup>

To study the effect of variation of Fe content on upper critical field,  $H_{c2}$  and irreversible field,  $H_{irr}$  the temperature dependence of resistivity in the superconducting transition region has been measured in applied magnetic fields in the range 0–8 T. The field dependent transitions of sample  $x = 1.00$  are shown in the inset of Fig. 2. From the field dependent  $\rho$ - $T$  plots it has been found that critical temperature  $T_c$  shifts toward lower temperature with the application of magnetic field, indicating the suppression of superconductivity on applying magnetic field.  $H_{c2}(T)$  and  $H_{irr}(T)$  are estimated using the criterion 90% and 10% of normal state resistivity  $\rho_n(H,T)$ , respectively. In Fig. 3, we plot both  $H_{c2}$  and  $H_{irr}$  as a function of temperature. The upper critical field at 0 K,  $H_{c2}(0)$  has been estimated using the Werthamer-Helfand-Hohenberg (WHH) formula,<sup>15</sup>  $H_{c2}(0) = -0.693 T_c (\partial H_{c2} / \partial T)_{T_c}$ .

The values of  $H_{c2}(0)$  thus calculated are 121 T, 142 T, 87 T, and 79 T, respectively for  $x = 0.95, 1.00, 1.05,$  and  $1.10$ . The decreased values of  $H_{c2}(0)$  for  $x = 1.05$  and  $1.10$

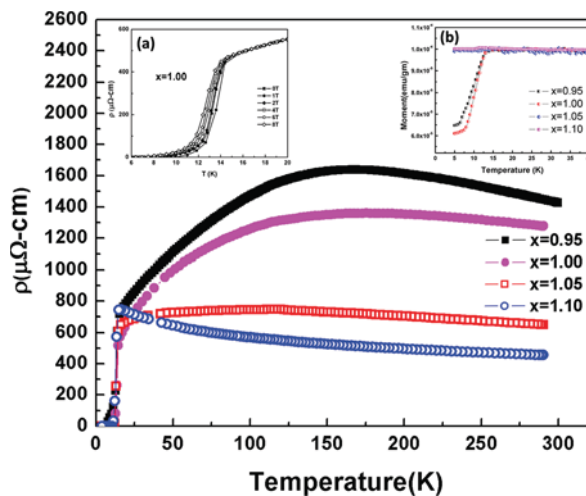


FIG. 2. (Color online) Temperature dependence of resistivity in zero magnetic field in the temperature range 300–4 K for all samples. Inset (a) shows the temperature dependence of resistivity for  $x = 1.00$  in magnetic fields (0–8 T) and inset (b) shows temperature dependence of magnetization measurement (FC) of the samples in an applied field of 30 Oe.

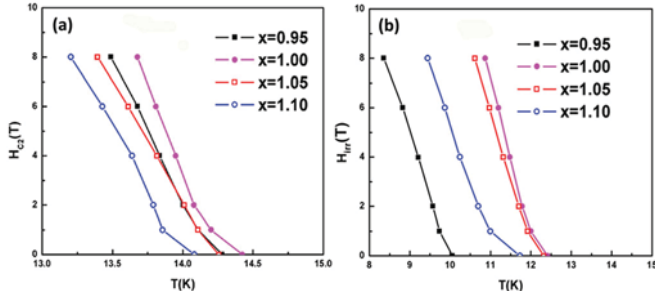


FIG. 3. (Color online) Temperature dependence of  $H_{c2}$ , (a) and  $H_{irr}$ , (b) for  $\text{Fe}_x\text{Se}_{1/2}\text{Te}_{1/2}$  ( $x = 0.95, 1.00, 1.05, \text{ and } 1.10$ ).

may be correlated with the strong disorder induced by introducing excess iron in the conducting layer. From  $H_{c2}(0)$ , zero-temperature coherence length  $\xi(0)$  can be calculated using GL formula,<sup>16,17</sup>  $H_{c2}(0) = \phi_0 / (2\pi\xi^2(0))$ . The estimated values of  $\xi(0)$  are 17, 15.5, 20, and 20.4 Å, respectively for  $x = 0.95, 1.00, 1.05, \text{ and } 1.10$ .

The superconducting transition width is  $\sim 2$  K for all the samples except for  $x = 0.95$  for which it is  $\sim 4$  K. The higher value of transition width for  $x = 0.95$  is possibly due to the presence of more impurity phases, as seen from XRD result, causing large scattering centers. Furthermore, the broadening in the transition increases with the application of magnetic field. This magnetoresistive broadening can be ascribed to the TAFF of the vortices. The activation energy for this TAFF is found using the Arrhenius law,<sup>17–19</sup>  $\rho = \rho_0 \exp(-U_0/K_B T)$ , where  $\rho_0$  is the normal state resistivity and  $U_0$  is the activation energy of the flux flow. In Fig. 4, we show the Arrhenius plot of the resistivity ( $\log \rho$  versus  $100/T$ ) with applied magnetic fields. The straight part above the  $T_c^{zero}$  of the  $\log \rho - 100/T$  curves represents the TAFF regime and its slope gives the value of activation energy  $U_0$  of flux-flow. The linear fitting of the experimental data gives the values of  $U_0$  ranging between 25 and 91 K for  $x = 0.95 - 1.10$  in magnetic field of 1 T and between 15 and 60 K in magnetic field of 8 T. The small values of activation energy in comparison to cuprates, indicates very small intrinsic pinning in these compounds. The order of magnitude of  $U_0$  is similar to the reported for other such materials.<sup>20</sup> We

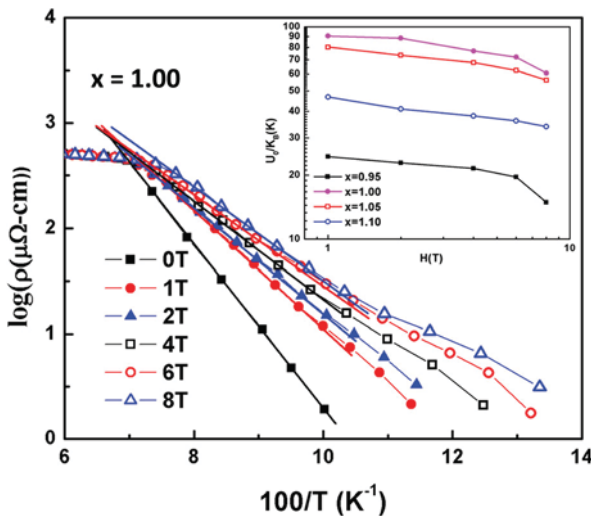


FIG. 4. (Color online) Arrhenius plot for the sample  $\text{Fe}_{1.00}\text{Se}_{1/2}\text{Te}_{1/2}$ . Inset shows the activation energy behavior in magnetic field.

also observe that the variation of  $H_{irr}$  with  $x$  is similar to the variation of  $U_0$  with  $x$  at a particular magnetic field. This suggests that pinning of flux lines first increases with  $x$  up to  $x = 1.00$  and then after it starts decreasing with increasing  $x$ .

#### IV. CONCLUSIONS

To conclude, we have found that the superconducting properties of the compound,  $\text{Fe}_x\text{Se}_{1/2}\text{Te}_{1/2}$  depend strongly on the Fe content. In the present case highest values of  $T_c^{zero}$ ,  $H_{c2}(0)$ , and  $H_{irr}$  have been found for  $x = 1.00$ . The excess iron present at the octahedral sites donates electron to the FeSe/Te site, due to which normal state resistivity decreases. The observed logarithmic behavior for the composition  $x = 1.10$  indicates the formation of localized electronic states with increased Fe content in  $\text{Fe}_x\text{Se}_{1/2}\text{Te}_{1/2}$ . The disorder created in the conducting layers gives rise to decreased activation energy and hence increased penetration depth.

#### ACKNOWLEDGMENTS

The financial supports from D.S.T. (Government of India) and M.H.R.D. (Government of India) are highly acknowledged.

- <sup>1</sup>Y. Kamihara, T. Watanabe, M. Hirano, and H. Hosono, *J. Am. Chem. Soc.* **130**, 3296 (2008).
- <sup>2</sup>M. Rotter, M. Tegel, D. Johrendt, I. Schellenberg, W. Hermes, and R. Pottgen, *Phys. Rev. B* **78**, 020503 (2008).
- <sup>3</sup>C. W. Chu, R. P. Chaudhury, F. Chen, M. Gooch, A. Guloy, B. Lorenz, B. Lv, K. Sasmal, Z. Tang, L. Wang, and Yu-Yi Xue, *J. Phys. Soc. Jpn., Suppl. C* **77**, 72 (2008).
- <sup>4</sup>J. H. Tapp, Z. Tang, B. Lv, K. Sasmal, B. Lorenz, P. C. W. Chu, and A. M. Guloy, *Phys. Rev. B* **78**, 060505(R) (2008).
- <sup>5</sup>F. C. Hsu, J. Y. Lup, K. W. Yeh, T. K. Chen, T. W. Huang, P. M. Y. C. Lee, Y. L. Huang, Y. Y. Chu, D. C. Yan D, and M. K. Wu, *Proc. Nat. Acad. Sci.* **105**, 14262 (2008).
- <sup>6</sup>J. Guo, S. Jin, G. Wang, S. Wang, K. Zhu, T. Zhou, M. He, and X. Chen, *Phys. Rev. B* **82**, 180520 (2010).
- <sup>7</sup>A. Subedi, L. Zhang, D. J. Singh, and M. H. Du, *Phys. Rev. B* **78**, 134514 (2008).
- <sup>8</sup>Y. Mizuguchi, F. Tomioka, S. Tsuda, T. Yamaguchi, and Y. Takano, *J. Phys. Soc. Jpn.* **78**, 074712 (2009).
- <sup>9</sup>W. Bao, Y. Qiu, Q. Huang, M. A. Green, P. Zajdel, M. R. Fitzsimmons, M. Zhernenkov, S. Chang, M. Fang, B. Qian, E. K. Vehstedt, J. Yang, H. M. Pham, L. Spinu, and Z. Q. Mao, *Phys. Rev. Lett.* **102**, 247001 (2009).
- <sup>10</sup>R. Viennois, E. Giannini, D. van der Marel, and R. Cerny, *J. Solid State Chem.* **183**, 769 (2010).
- <sup>11</sup>R. Shipra, H. Takeya, K. Hirata, and A. Sundaresan, *Physica C* **470**, 528 (2010).
- <sup>12</sup>T. J. Liu, X. Ke, B. Qian, J. Hu, D. Fobes, E. K. Vehstedt, H. Pham, J. H. Yang, M. H. Fang, L. Spinu, P. Schiffer, Y. Liu, and Z. Q. Mao, *Phys. Rev. B* **80**, 174509 (2009).
- <sup>13</sup>M. Bendele, P. Babkevich, S. Katrych, S. N. Gvasaliya, E. Pomjakushina, K. Conder, B. Roessli, A. T. Boothroyd, R. Khasanov, and H. Keller, *Phys. Rev. B* **82**, 212504 (2010).
- <sup>14</sup>L. Zhang, D. J. Singh, and M. H. Du, *Phys. Rev. B* **79**, 012506 (2009).
- <sup>15</sup>X. Wang, S. R. Ghorbani, G. Peleckis, and S. Dou, *Adv. Mater.* **21**, 236 (2009).
- <sup>16</sup>I. Pallecchi, C. Fanciulli, M. Tropeano, A. Palenzona, M. Ferretti, A. A. Malagoli, Martinelli, I. Sheikin, M. Putti, and C. Ferdeghini, *Phys. Rev. B* **79**, 104515 (2009).
- <sup>17</sup>D. Bhoi, L. S. Sharath Chandra, P. Choudhury, V. Ganesan, and P. Mandal, *Supercond. Sci. Technol.* **22**, 095015 (2009).
- <sup>18</sup>T. T. M. Palstra, B. Batlogg, R. B. Van Dover, L. F. Schneemeyer, and J. V. Waszczak, *Phys. Rev. B* **41**, 6621 (1990).
- <sup>19</sup>X. L. Wanga, A. H. Li, S. Yu, S. Ooi, K. Hirata, C. T. Lin, E. W. Collings, M. D. Sumption, M. Bhatia, S. Y. Ding, and S. X. Dou, *J. Appl. Phys.* **97**, 10B114 (2005).
- <sup>20</sup>S. Pandya, S. Sherif, L. S. S. Chandra, and V. Ganesan, *Supercond. Sci. Technol.* **24**, 045011 (2011).